LEGIBILITY NOTICE

A major purpose of the Technical Information Center is to provide the broadest dissemination possible of information contained in DOE's Research and Development Reports to business, industry, the academic community, and federal, state and local governments.

Although a small portion of this report is not reproducible, it is being made available to expedite the availability of information on the research discussed herein.

LA-UR -89-249

LA-UR--89-249

DE89 006555

Los Alamos National Laboratory is operated by the University of California for the United States Department of Energy under contract W-7405-ENG-36

Received by OSTI

FEB 0 6 1989

TITLE SHEAR BANDING IN TITANIUM WITH CONTROLLED ELONGATIONS AT 10^6/SEC.

AUTHOR(S) KARL P. STAUDHAMMER, MST-?
ALTON G. GRAY, MST-7

SUBMITTED TO Fourth International Conference on Mechanical Properties of Materials at High Rates of Strain
Oxford, England
March 20-22, 1989

MASTER

Los Alamos National Laboratory
Los Alamos, New Mexico 87545

Shear Banding in Titanium with Controlled Elongations at 10^6/sec

K.P. Staudhammer* and A.J. Gray

Materials Science and Technology Division, Los Alamos National Laboratory, Los Alamos, NM 87545

*Currently on sabbatical leave as a U.S. Senior Scientist Awardee from the Alexander von Humboldt Stiftung at the Fraunhofer-Institut für Angewandte Materialforschung, Bremen, FRG.

ABSTRACT: Adiabatic shear bands were obtained in titanium with controlled strains to 10.8 %. Two types of shear bands were observed and characterized. In general the quantity and shear band width increased with increasing elongation. At elongations below ~ 5 % the shear bands were typically characteristic of shear bands observed at lower strain rates. Above 5 % elongations many of the shear bands contained a boundary regime adjacent to the shear band and increased in width with increasing total elongation. This effect was attributed to the strain heat.

1. INTRODUCTION

At high strain rates adiabatic shear localization is a very important phenomenon that has a profound effect on plastic deformation and fracture. Here we describe the first observations made of the nature of adiabatic shear bands in commercially pure titanium shock elongated at a strain rate of 10^6/sec.

Controlled strain experiments were achieved by the use of impedence matched pedestals of various heights which dictated the amount of the reflected tensile wave in the sample. This tensile wave imparts a certain degree of deformation in the sample, which in turn generates heat and thus promotes the formation of adiabatic shear bands. These shear bands have been documented by Rogers (1979) in a variety of bulk forming operations and for titanium alloys by Semiatin and Lahoti (1981 a,b). Until the present time, there has been no data on the shear band formation in titanium with high rate tensile deformation. For most experiments that have been done, the strain rate has been around 10^3/sec. or below and they were done primarily with titanium alloys such as that by Bryant and Wilsdorf (1988). Numerous publications exist for Ti and Ti-alloys examined under compression.

2. EXPERIMENTAL

Figure 1 illustrates the cylindrical arrangement for subjecting a solid bar specimen of titanium (purity 99.7 %, all samples were from one lot) to continuously varying pressure along the specimen length from 7 to 95 GPa. In this arrangement, detonation of the main charge (composition C-4 ex-

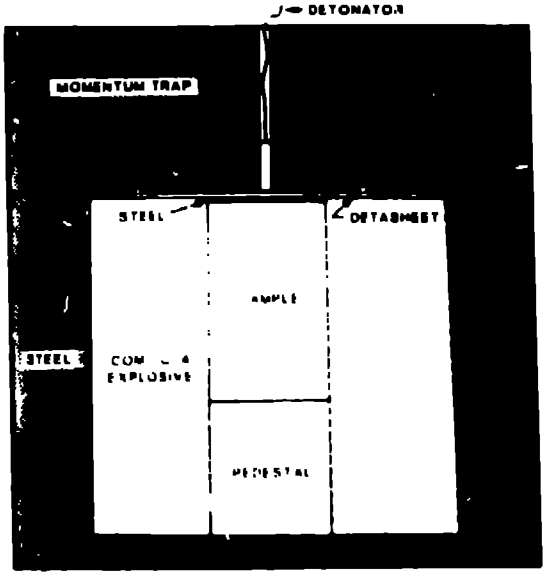

Fig. 1. Schematic of the shock loading assembly.

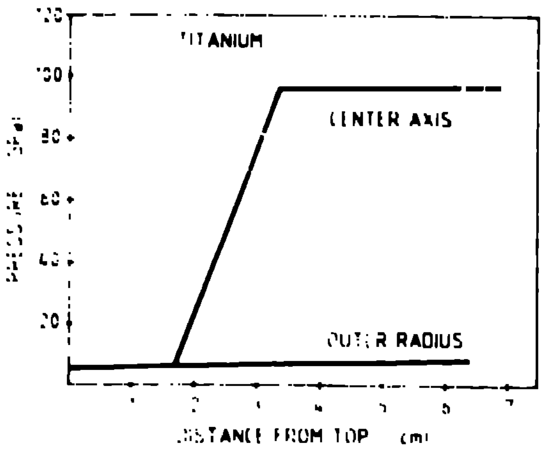

Fig. 2. Calculated pressure vs distance in titanium along central axis and outer radius of the test sample for C-4 explosives.

plosive) begins radially at the top edge of the specimen and as the detonation wave moves radially outward and downward, the pressure is added incrementally at a rapid rate. The key to accurately determining the pressure profile along the specimen, and the shock wave profile within the specimen, is a two-dimensional Eulerian computer code in use at Los Alamos National Laboratory. For titanium, this profile is shown in Fig. 2. Annealed solid cylindrical samples utilized in the arrangement shown schematically in Fig. 1 had an initial grain size of 50 μm, and a corresponding microhardness of 240 VHN. The samples were 63.4 mm in length and 38.1 mm in diameter.

The technique for strain measurements is based on circle griding. A network of circle grids were photoplated onto the preshocked specimen. The estimated accuracy for post shock local strain measurement is 1%. These grids could then be post shock measured for both lateral and vertical strain at each circle position. The griding technique is described elsewhere by Hecker (1978). With knowledge of local strain and calculated pressure, optical microscopy was made and referenced to known shock variables. Specimens for optical microscopy were cut both parallel and perpendicular to the cylinder axis so that comparisons of the residual microstructures could be made.

It should be noted from the shock wave profile which travels through the cylindrical specimen, that it is by comparison to a plane compressive wave, a shear wave making an angle of 45° with the specimen central axis. This shock-wave geometry, and the associated specimen deformation, produces a triaxial stress state which is tantamount to a high strain rate extrusion in the arrangement shown in Fig. 1. The actual strain rates, which can be deduced from the computer codes, were in the range of 10^6/sec.

3. RESULTS

The use of a pedestal as shown in Fig. 1 enabled variations of elongation between [illegible].5 to 14 % (fracture) to be achieved in titanium. This was based on earlier work on 304 stainless steel by Johnson et al (1986) and Staudhammer et al (1986).

3.1 Strain effect

Different strain values were obtained by varying the pedestal height. The top momentum trap was concomitantly adjusted to match the height of the pedestal to ensure 100 % recovery. The amount of elongation from separate experiments versus the pedestal height is plotted in Fig. 3, along with the results from similar experiments for 304 stainless steel. Both titanium and 304 stainless steel follow the same trend, ie, by increasing the pedestal height, a reduction of the overall strain is achieved. The minimum elongation achieved in titanium was 4.9 %. A post shocked sample using this pedestal design is shown in Fig. 4. Observed in this figure are two types of shear bands, a radial cone and a more classical tangential axisymmetric geometry. They both can be segmented and with the radial type being generally associated with the higher strains. These will be discussed later. The overall elongation in the sample increases from the top to the bottom and was varied by the pedestal height. Additionally, at any point along the cylindrical axis the strain is essentially uniform across the diameter for homogeneously deformed materials as shown by Staudhammer

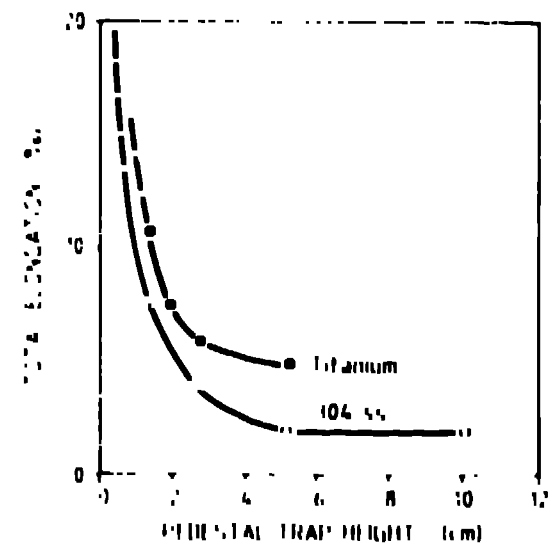

Fig. 3. Overall elongation vs pedestal height for C-4 explosive.

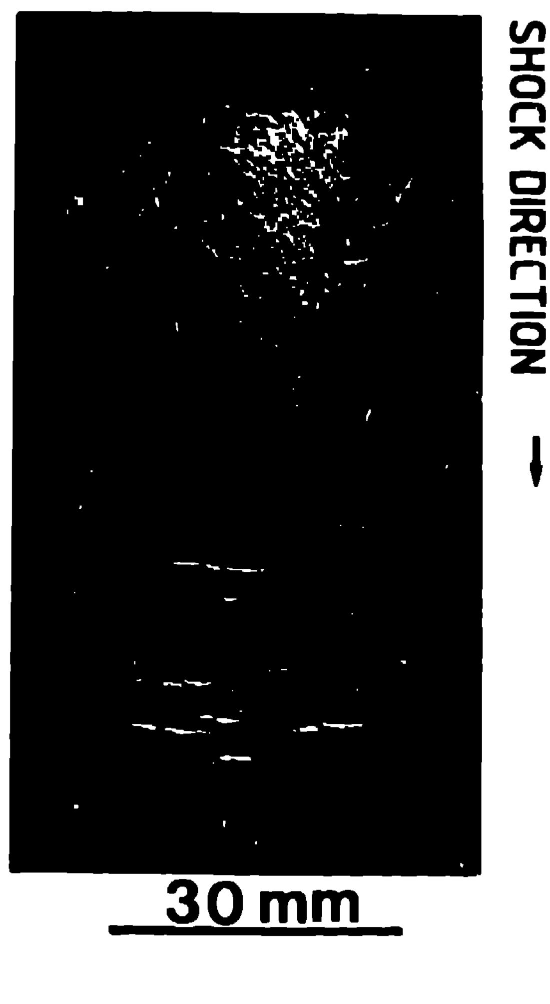

Fig. 4. Photograph of titanium post shocked sample, elongation 4.9 %.

and Johnson (1958). Titanium which has a preference for flow localization, has tensile elongation characteristics as shown in Fig. 5. In this figure, three controlled elongation experiments are shown for pedestal heights of 2.1 cm yielding an overall total strain of 4.9 %, 1.9 cm yielding 7.2 % and, 1.3 cm yielding 13.5 %. The observed shear bands are shown as dashed lines. The shear band locations indicated in Fig. 5 are the locations observed on the outer surface along the axial length of each specimen.

The local strain (measured from circle grids) between shear band segments, ie, the plateau steps on each of the samples, irrespective of the overall elongation, had little if any measureable strain. All local strain readings were within the lower limit of the grid technique and did not exceed 1 %.

2.2 Pressure temperature effects

Shock pressures at essentially zero strain produce two temperature effects. The adiabatic temperature pulse and the residual temperature. Both of these temperatures are a function of pressure and they were first published by Rice et al (1958), McQueen et al (1960) and McQueen et al (1970), for a variety of materials. By including strain in the system, the deformation heat must be added in. At this point one must keep in mind that these temperatures are in fact what the sample "sees". They however, do not occur at the same time. This perhaps can best be illustrated schematically in Figure 6. Shown here is a temperature-time profile at a given position and pressure in the sample. The temperature ΔT_A and ΔT_r are established by the shock pressure, and ΔT_ε is determined by the strain magnitude. The adiabatic temperature rise ΔT_A exists for approximately 1 µs and leaves with the pressure pulse (pulse duration), the residual temperature rise ΔT_r exists in the sample right after the release of the adiabatic temperature and is a long term effect. The strain heat ΔT_ε appears in the sample at a time which is twice the travel distance from the point of interest and the reflecting free surface times, the shock velocity in

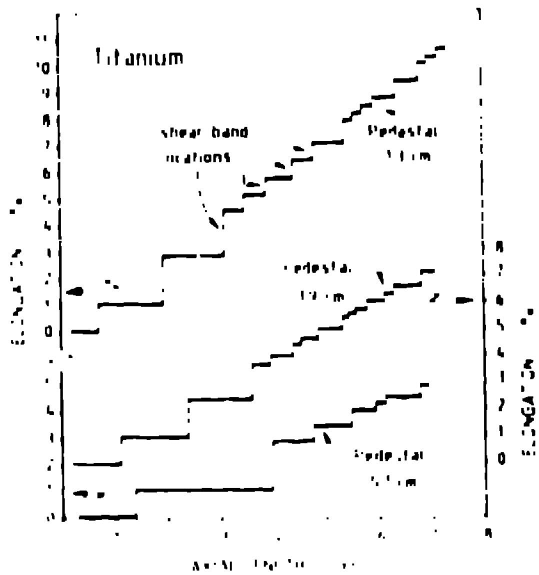

Fig. 5. Total elongation vs axial length for 3 pedestal heights.

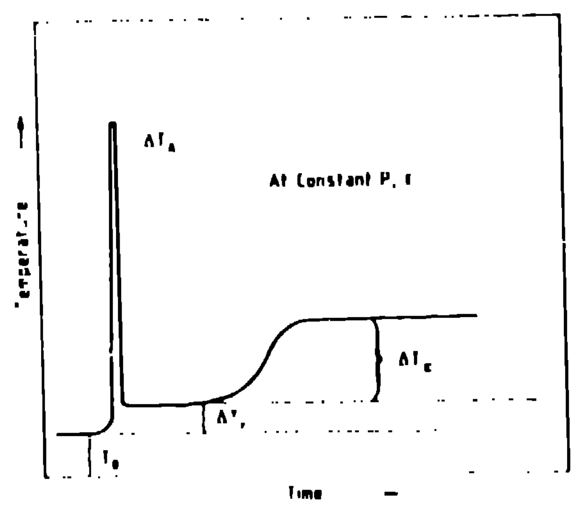

Fig. 6. Relationship of the adiabatic, residual and strain temperatures vs time for a given pressure and position in the sample.

titanium. While the pulse duration for ΔT_A is 1 μs, the distances from the reflecting surface can exceed 6 cm. Consequently, one must look more closely at the time separation of the adiabatic and strain temperatures. The adiabatic temperature results from a shock compression wave which is a function of pressure and can be obtained from the data of McQueen et al (1970). The strain temperature results from the tensile reflected wave and as such, they only overlap at the free surface where the strain temperature component is initiated. As the tensile reflected wave propagates back through the shocked sample, the time delay between the adiabatic and strain temperature gets larger. This results in a time delay of from near 0 μsec. at the bottom of the sample to approximately 11 μsec. at the top of the sample. The pedestal not only controls the amount of the overall elongation, it also increases the delay time between the adiabatic and strain temperatures since this is proportional to the pedestal height. For a 1.3 cm pedestal, this results in a delay time of near 3 μsec. and for a 7 cm pedestal, near 10 μsec. This time delay insures that the adiabatic and strain temperatures are separate and do not occur simultaneously.

Until now, all the figures shown referred to axial lengths in the sample. To obtain a better picture one must observe the radial cross sections as well. This is illustrated in Fig. 7. Shown in Fig. 7a is the radial pressure profile at 5 cm from the top of the sample (see Fig. 2), and is calculated from data after McQueen et al (1970). Strain measurements are shown in Fig. 7b, for the 10.6 % elongated sample. The local strains in the bulk are relatively low. However, in the shear bands the local strains are significantly larger. The values as shown, where obtainable, are only approximate and estimated from shear offsets, as the cross section of the sample was not grided. These strain values do, however, represent the trend across the cross section with the shear bands decreasing in magnitude towards the center of the sample. This was observed in all samples, particularly in the high strain regions. This is in contrast to what is observed in a homogeneously deformed sample such as 304 stainless steel under similar conditions as shown by Staudhammer and Johnson (1988) where the strain across the sample diameter at any position was constant and not related to the pressure profile. The temperature profiles are shown in Fig. 7c. All temperatures except the strain temperature are known or calculated values. The strain temperatures are schematically illustrated.

An additional pressure effect that should be addressed is that of shock hardening. Shock hardening results from a shock event which induces microstructural changes that are governed by the same basic features which govern all deformation microstructures. In materials such as titanium in which shear bands are easily obtained, the deformation is highly localized in the shear band and relatively unaffected in the matrix. Microhardness measurements were made for all regimes of elongation including shear bands and matrix. All the post shocked readings had essentially the same value which averaged 333 VHN for all three elongations. This is not inconsistent with other observations made on titanium alloys by Jonas (1978). The shock did, however, increase the overall hardness from the as received annealed condition which had a value of 240 VHN.

3.3 Shear band characteristics

As indicated earlier, two types of shear bands are observed. One that intersects the outside diameter at an angle of 45° to the axial length of the sample and is observed over the length of the sample (ie occurs at all levels of elongation). The second type of shear band had a radial cone

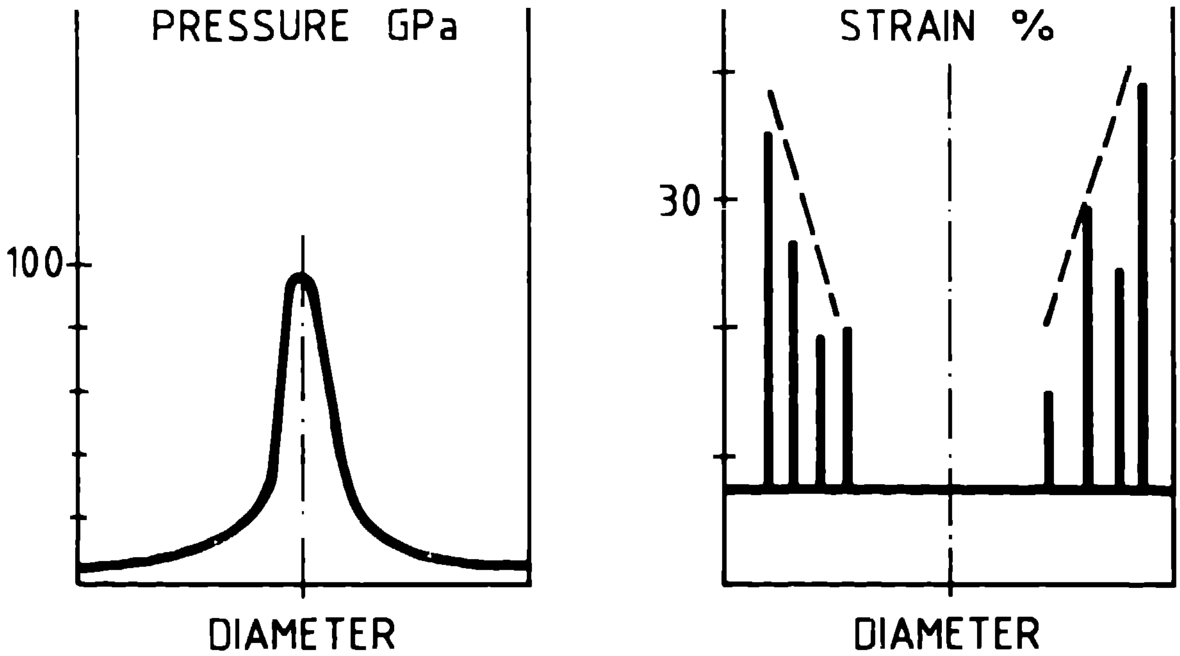

Fig. 7. Relationship of
a) pressure b) local strain and
c) associated temperature effects
across the diameter of a 3.5 %
elongated titanium sample.

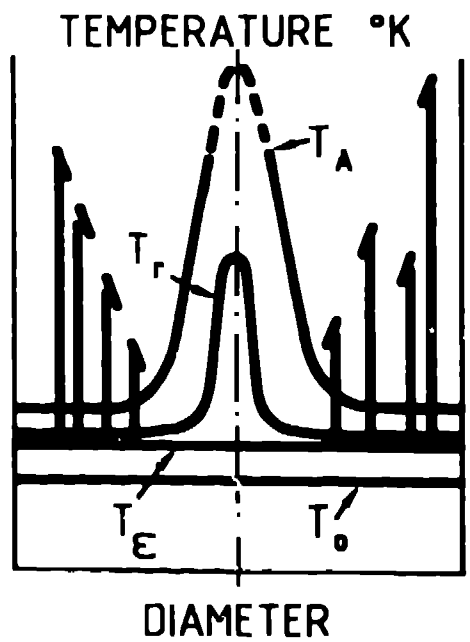

shape with a 45° intersection of the outside diameter and the cone apex. The microstructural characteristics of both types of shear bands are identical and appear to vary only in their geometry. These observations and descriptions have been observed in the work of Staker (1981), Culver (1973) and Semiatin et al (1984) where shear localization in the shear band occurs by simple shear.

Typical microstructures are shown in Fig. 8a for the axial length type and is from a longitudinal section. Figure 8b for the radial cone type is from a radial cross section. Figure 8a is from a region of low strain (2 cm from the top of the sample) and Fig. 8b from a region of higher

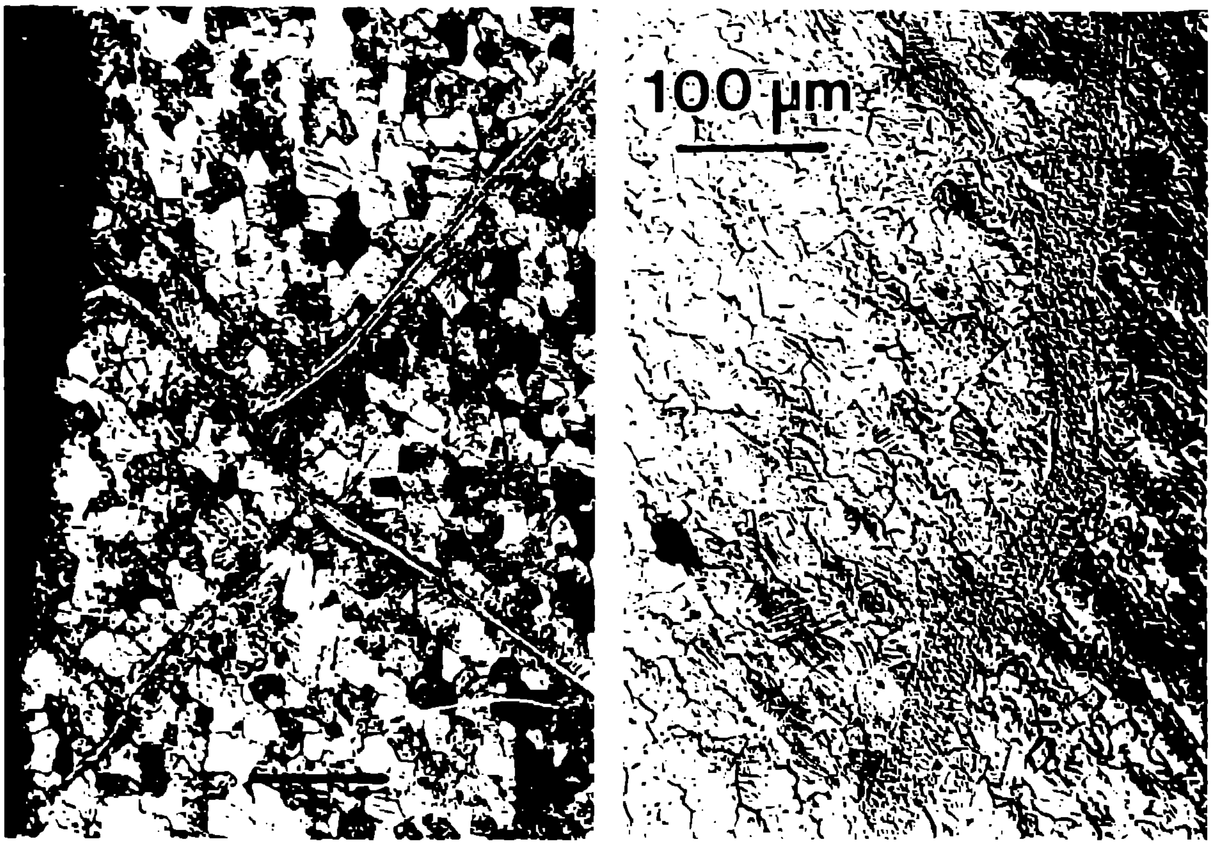

Fig. 8. Shear bands in titanium shocked at 10^6/s a) from a longitudinal section at an elongation of 1 %, b) from a radial cross section at an elongation of 5 %. Micrographs a), b) from the 5 cm pedestal shot. Figure 8b was obtained by differential interference contrast by Nomarski techniques.

Fig. 9. Typical shear band microstructure in the high strain region of titanium. Note the heat affected zone adjacent to the shear band.

strain (5 cm from the top). The high strain region in all three samples had for the larger shear bands the characteristics shown in Fig. 9. As this is the high pressure region, as well as the higher strain region, the temperature in this regime will be the highest in the sample. Similarly the time delay between adiabatic and strain temperatures is the shortest and as such would have the greatest effect on thermal softening of the sample.

4. CONCLUSION

- Shear bands occuring at 10^6/s and appearing to be independent of shock pressure, are dominated by strain and have the same character as those observed at lower strain rates.

- The number of shear bands increases with overall elongation. Similarly the width of the shear band generally increases with increased overall elongation.

- Shock hardening was observed in the bulk, however the shear bands had the same hardness. This is due to the annealing effects of the strain heat in the shear band, particularly at large strains.

5. REFERENCES

Bryant J D and Wilsdorf H G F 1988 Impact Loading and Dynamic Behaviour of Materials ed C Y Chiem et al (Verlag Informationsgesellschaft) pp 145-152

Culver R S 1973 Metallurgical Effects at High Strain Rates (New York, Plenum Press) pp 519

Johnson K A and Staudhammer K P 1986 Metall. Applications of Shock-Wave and High-Strain-Rate Phenomena ed L E Murr and M A Meyers (New York, Dekker) pp 525

Jonas J J and Luton M J 1978 Advances in Def. Procc. (New York, Plenum) pp 215

McQueen R G and Marsh S P 1960 J.A.P. 31 1253

McQueen R G et al 1970 High-Velocity Impact Phenomena (New York, Academic Press) pp 293

Rice M H, McQueen R J and Walsh J M 1958 Solid State Physics 6 (New York, Academic Press) pp 1

Rogers H C 1979 Ann. Rev. Mat. Sci. 9 283

Semiatin S L and Lahoti G D 1981a Met. Trans. 12A 1705

Semiatin S L and Lahoti G D 1981b Met. Trans. 12A 1719

Semiatin S L et al 1984 Acta Met. 32 1347

Staudhammer K P and Johnson K A 1986a Proc. of the Intl. Symp. on Intense Dynamic Loading and its Effects ed C M Cheng and D Jing (Beijing, Science Press) pp 759

Staudhammer K P and Johnson K A 1988b Impact Loading and Dynamic Behaviour of Materials (Verlag Informationsgesellschaft) pp 839

Staker M R 1981 Acta Met. 29 683